




Please cite the Published Version

Garg, Saweta, Singla, Pankaj, Kaur, Sarbjeet, Crapnell, Robert D , Banks, Craig E , Seyedin, Shayan and Peeters, Marloes  (2024) Electroactive Molecularly Imprinted Polymer Nanoparticles (eMIPs) for Labelfree Detection of Glucose: Toward Wearable Monitoring. *Small*. 2403320
ISSN 1613-6810

DOI: <https://doi.org/10.1002/sml.202403320>

Publisher: Wiley

Version: Published Version

Downloaded from: <https://e-space.mmu.ac.uk/635504/>

Usage rights:  [Creative Commons: Attribution 4.0](https://creativecommons.org/licenses/by/4.0/)

Additional Information: This is an open access article which first appeared in *Small*, published by Wiley

Data Access Statement: The data that support the findings of this study are available in the supplementary material of this article.

Enquiries:

If you have questions about this document, contact openresearch@mmu.ac.uk. Please include the URL of the record in e-space. If you believe that your, or a third party's rights have been compromised through this document please see our Take Down policy (available from <https://www.mmu.ac.uk/library/using-the-library/policies-and-guidelines>)

Electroactive Molecularly Imprinted Polymer Nanoparticles (eMIPs) for Label-free Detection of Glucose: Toward Wearable Monitoring

Saweta Garg, Pankaj Singla, Sarbjeet Kaur, Robert D. Crapnell, Craig E. Banks, Shayan Seyedin,* and Marloes Peeters*

The diagnosis of diabetes mellitus (DM) affecting 537 million adults worldwide relies on invasive and costly enzymatic methods that have limited stability. Electroactive polypyrrole (PPy)-based molecularly imprinted polymer nanoparticles (eMIPs) have been developed that rival the affinity of enzymes whilst being low-cost, highly robust, and facile to produce. By drop-casting eMIPs onto low-cost disposable screen-printed electrodes (SPEs), sensors have been manufactured that can electrochemically detect glucose in a wide dynamic range (1 μM –10 mM) with a limit of detection (LOD) of 26 nM . The eMIPs sensors exhibit no cross reactivity to similar compounds and negligible glucose binding to non-imprinted polymeric nanoparticles (eNIPs). Measurements of serum samples of diabetic patients demonstrate excellent correlation (>0.93) between these eMIPs sensor and the current gold standard Roche blood analyzer test. Finally, the eMIPs sensors are highly durable and reproducible (storage >12 months), showcasing excellent robustness and thermal and chemical stability. Proof-of-application is provided via measuring glucose using these eMIPs sensor in a two-electrode configuration in spiked artificial interstitial fluid (AISF), highlighting its potential for non-invasive wearable monitoring. Due to the versatility of the eMIPs that can be adapted to virtually any target, this platform technology holds high promise for sustainable healthcare applications via providing rapid detection, low-cost, and inherent robustness.

worldwide.^[1] According to the International Diabetes Federation, over 537 million adults (aged 20–79) had diabetes in 2021 with projections indicating a rise to 643 million by 2030.^[2,3] Moreover, high blood sugar (>7 mM) in diabetes can damage tissues resulting in comorbidities such as renal failure, retinopathy, neuropathy, and cardiovascular and cerebrovascular diseases.^[4,5] Therefore, it is crucial to develop a rapid and precise glucose sensing platform to effectively manage, monitor, and mitigate the progression of diabetes and its related complications.^[6,7] The alarming increase in global incidence of diabetes has spurred a significant expansion in the market for glucose biosensors. In 2022, the global market for glucose biosensors was valued at US\$12.9 billion which is projected to rise exponentially to US\$40 billion by 2032.^[8]

Over the last 50 years, finger-prick glucose testing, relying on enzymes such as glucose oxidase, has remained the preferred method for the majority of individuals with diabetes.^[9] However, this method is invasive and often leads to non-compliance among patients who need to undergo multiple finger pricks throughout the day to manage their glucose levels. Furthermore, the interference with certain substances present in blood, such as galactose, fructose, and ascorbic acid, also affects the accuracy of testing.^[9,10] Enzyme-based sensors have been used for many years due to

1. Introduction

Diabetes mellitus (DM) has been established as a common, chronic metabolic syndrome and is the 9th leading cause of death

S. Garg, P. Singla, M. Peeters
Department of Chemical Engineering
The University of Manchester
Engineering building A, East Booth Street, Oxford Road, Manchester
M13 9PL, UK
E-mail: marloes.peeters@manchester.ac.uk

 The ORCID identification number(s) for the author(s) of this article can be found under <https://doi.org/10.1002/smll.202403320>

© 2024 The Author(s). Small published by Wiley-VCH GmbH. This is an open access article under the terms of the [Creative Commons Attribution License](https://creativecommons.org/licenses/by/4.0/), which permits use, distribution and reproduction in any medium, provided the original work is properly cited.

DOI: 10.1002/smll.202403320

S. Garg, P. Singla, S. Kaur, S. Seyedin
School of Engineering
Newcastle University
Newcastle upon Tyne NE1 7RU, UK
E-mail: shayan.seyedin@ncl.ac.uk
S. Kaur
Department of Chemistry
Centre for Advanced Studies
Guru Nanak Dev University
Amritsar, Punjab 143005, India
R. D. Crapnell, C. E. Banks
Faculty of Science and Engineering
Manchester Metropolitan University
Manchester M1 5GD, UK

their excellent selectivity and sensitivity.^[11] However, they pose significant challenges such as poor stability (<6 months and requiring storage at low temperatures, i.e., 4 °C), limited shelf life, and low tolerance against environmental conditions (e.g., loss of activity above 40 °C).^[12,13] Non-invasive sampling methods, such as sweat and saliva-based analysis, are gaining popularity as alternative options to finger prick tests due to improving patient comfort.^[14] Enzymatic sensors currently face challenges in achieving adequate sensitivity due to the susceptibility of glucose oxidase to deactivation for detecting low glucose levels in non-invasive samples. Non-enzymatic sensors have also been widely explored which typically utilize transition metal-based nanomaterials, noble metals, or non-noble transition metals as synthetic receptors.^[15] However, such sensors are costly due to the use of metals or require harsh electrolyte conditions (alkaline media, pH>11) to work, which do not facilitate direct blood sample measurements without significant sample pre-treatment.^[16,17] Recently, wearable glucose sensors have emerged as a viable alternative to existing finger prick sensors due to their real-time continuous monitoring capabilities and convenience for frequent testing but are still invasive and expensive.^[18,19] Furthermore, due to the correlation of the blood glucose level with that in other fluids including interstitial fluid (ISF), wearable sensors for glucose testing in ISF offer a potential alternative to traditional finger prick tests.^[20,21] For instance, Dexcom G6 and Abbott Free Style Libre are the popular continuous glucose monitoring systems in ISF but they are not accessible to the most of the population due to its high-cost (for instance, Dexcom G6 costs \$237 for G6 transmitter and \$349 for a three-pack of sensors) and limited lifetime of two weeks.^[22–24]

One promising approach to reducing the costs of the wearable glucose sensors is to replace enzymes with alternative recognition elements. Molecularly imprinted polymers (MIPs) are promising synthetic receptors that have been employed for the development of robust and inexpensive electrochemical sensors due to their high specificity for the chosen template.^[25,26] MIPs are porous materials containing high affinity binding for their respective targets and have gained significant interest due to their economical and straightforward preparation, reusability, robustness, biocompatibility, versatility, and specific target recognition in complex matrices.^[27,28] Previous literature reports demonstrated that several molecules including different biomarkers (lipids, proteins, and serum amyloid A), glucose, and interleukin-6 can be molecularly imprinted within conventional (i.e., non-electroactive) polymers via electrochemical detection.^[29–31] Electrochemical measurements have gained widespread use in glucose monitoring due to their high sensitivity, excellent selectivity, and straightforward operation. For instance, polypyrrole (PPy) among other conductive polymers, has been widely utilized in the fabrication of electroactive MIPs (eMIPs) based sensors since it offers a high electrical conductivity ($\approx 10^5$ S cm⁻¹), environmental stability, long term stability (≥ 1 year), and straightforward polymerization procedure.^[32–34] PPy-based eMIPs sensors have been used for the electrochemical detection of different small and large molecules or drugs such as ethanethiol, L-tryptophan, SARS-CoV-2 spike glycoprotein, and *Klebsiella pneumoniae*, showed excellent selectivity, sensitivity, and a low limit of detection (LOD) in real samples.^[35–37] However, most studies on PPy-based eMIPs sensors employed a synthesis method that involved direction de-

position of the MIP layer on the surface. This often results in a low utilization of imprinted cavities, non-uniformity of the layer, and slow adsorption rates, thus leading to poor reproducibility and limiting commercial scalability.^[37]

Conventional electrodes such as glassy carbon, platinum, and gold, and have been widely used for the development of eMIPs based glucose electrochemical sensor. However, current electrochemical methods often require a multi-step process involving the pretreatment with nanomaterials such as gold nanoparticles (AuNPs), graphene oxide, electro-polymerization of various monomers including aminophenylboronic acid (APBA), and pyrrole (Py) to achieve electrochemical sensing. Uygun et al. developed eMIPs-based glucose sensors by modifying bespoke platinum screen-printed electrodes (PtE) with electrochemical polymerization of APBA and Py.^[38] The sensor was used to detect glucose employing chronoamperometry exhibiting a LOD of 0.3 mM. Yang et al. also developed eMIPs based glucose sensor by electropolymerizing eMIPs micelles and achieved an upper detection limit of 10 mM. However, the eMIPs micelles were prepared using photo-crosslinkable amphiphilic copolymer which involved a complicated multistep manufacturing method.^[39] AuNPs coated MIPs were synthesized using free radical polymerization and electrodeposited on the gold (Au) electrodes in the presence of glucose as a template with a LOD of 3 pM.^[40] The development of the AuNPs-MIP-based glucose sensor involved a time consuming, tedious, and costly fabrication process that required cross-linking for electrodeposition, thus lacking scalability.

This work introduces an innovative enzyme free PPy-eMIPs nanoparticles based SPEs sensor for rapid electrochemical detection of glucose in both serum samples of diabetic patients and artificial interstitial fluid (AISF). The novel, straightforward, one-pot synthesis of eMIPs and deposition onto inexpensive SPEs (<\$0.1) eliminate the need for complex electrode modifications, offering significant cost reductions and scalability potential.^[41,42] We demonstrate the selective binding of glucose with eMIPs sensor with a LOD of ≈ 26 nM which is significantly lower compared to other glucose sensors (LOD of ≈ 0.3 M).^[43] Additionally, the unique electroconductivity of PPy-based eMIPs enables high sensitivity, fast response time (<30 s), high selectivity (no significant change in current with other sugars, ascorbic acid, and dopamine), and specificity (no response with control particles, i.e., non-imprinted polymers, eNIPs). The eMIPs sensors exhibit exceptional robustness as they could operate at extremes of temperature (20–120 °C), pH (5.0, 7.0, and 9.0) and possess long-term stability (≥ 360 days) at room temperature (RT). When used in a two-electrode setup, a LOD of 132 nM is achieved for glucose detection highlighting the potential for use in wearable applications. The eMIPs sensor is capable of determining glucose levels in spiked human serum (HS) samples and serum samples of different diabetic patients. Furthermore, we observed a strong correlation (correlation coefficient >0.9) between the results obtained from diabetic serum samples using our eMIPs sensor and those from the gold standard Roche blood analyzer. In addition, the ability of the developed eMIPs sensor to measure glucose levels in AISF samples (LOD ≈ 44 nM) with a high correlation (correlation coefficient = 0.99) to serum results, make it compatible with non-invasive monitoring through wearable technology. Overall, our approach offers versatility beyond traditional

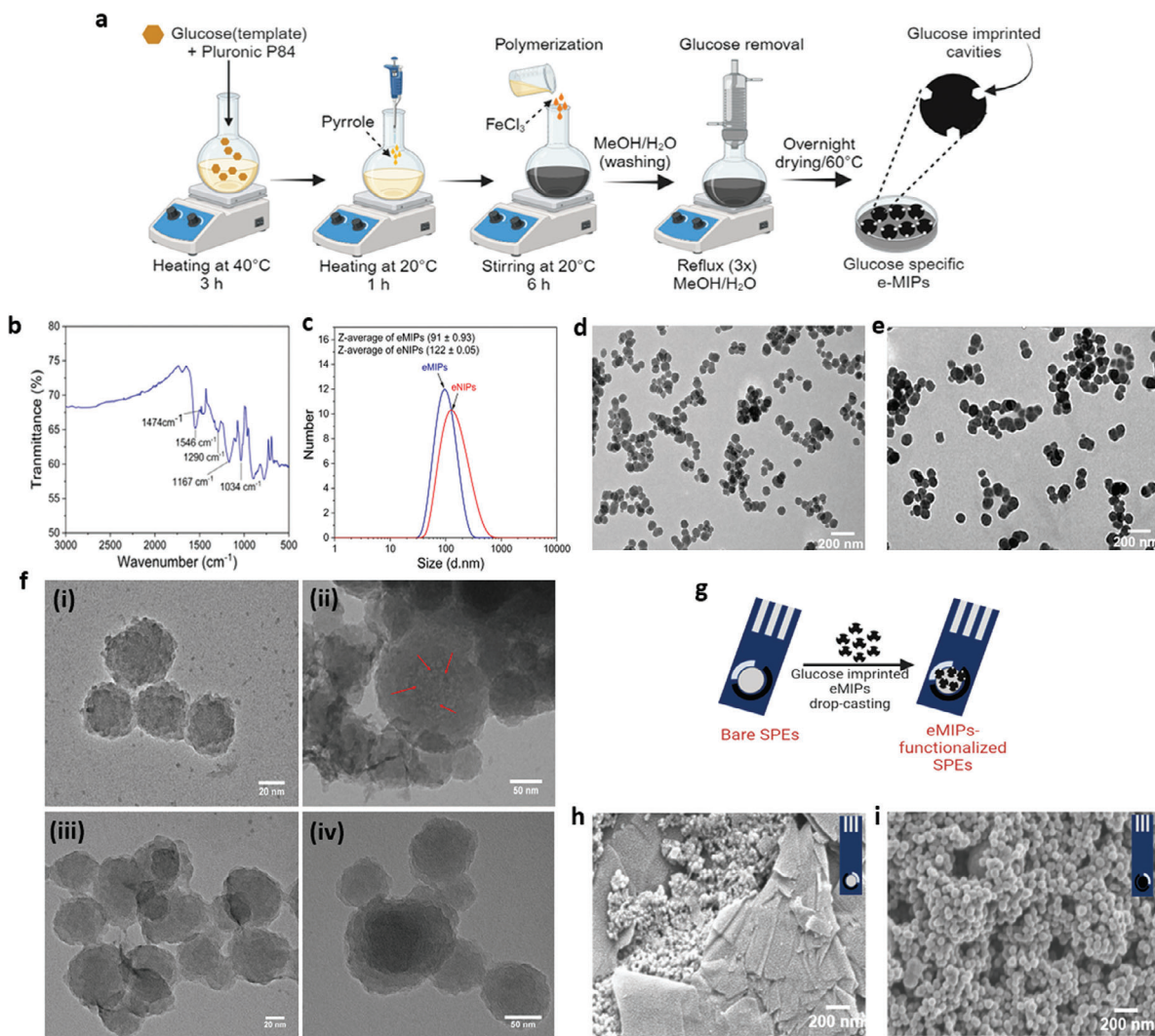


Figure 1. a) Schematic representation of the synthesis of glucose imprinted electroactive MIPs (eMIPs). b) FTIR spectrum of PPy-eMIP. c) eMIPs and non-imprinted polymer (eNIPs) particle size distribution (number versus size in nm) measured by dynamic light scattering (DLS). Transmission electron microscopy (TEM) images of d) eMIPs and e) eNIPs. f) TEM images of eMIPs (i and ii) and eNIPs (iii and iv) at high magnification (scale bar 20 and 50 nm). g) schematic representation of the preparation of eMIPs-functionalized SPEs (eMIPs-SPEs). Scanning electron microscopy (SEM) images of h) bare SPE and i) eMIPs-SPEs.

electrode substrates and its adaptability allows for comfortable, discreet, and user-friendly glucose monitoring solutions, catering to diverse needs of individuals managing diabetes. The high selectivity and versatility of the eMIP sensor, along with its ability to function in clinical samples, highlight its potential for detecting other biomarkers such as creatinine, urea, and dopamine. This will contribute to the advancement of wearable sensors for patients with multi-morbidities like chronic kidney and, coronary artery disease that require simultaneous monitoring.

2. Results and Discussion

2.1. Synthesis and Characterization of eMIPs

eMIPs have been produced through free-radical polymerization using Py as an electroactive monomer, glucose as a template,

and Pluronic P84 as a surface-active agent (Figure 1a). Similarly, eNIPs were synthesized employing the same synthesis method used for eMIPs synthesis without the addition of glucose (Particle Size and Morphology Characterization of eMIPs and eNIPs). The resulting eMIPs were characterized for their size, morphology, and imprinting using different techniques such as DLS, TEM, and FTIR spectroscopy. To confirm the synthesis of PPy, samples were characterized by FTIR (Figure 1b) and the results were in agreement with literature findings.^[44] The bands observed at 1546 and 1474 cm^{-1} were attributed to the fundamental vibrations of the PPy ring, while those at 1290 and 1034 cm^{-1} corresponded to the =C–H in-plane vibrations, and the band at 1167 cm^{-1} was associated with the C–N stretching vibrations. DLS results showed a hydrodynamic diameter (D_h) of 91 ± 0.9 and 122 ± 0.1 nm for eMIPs and eNIPs respectively (Figure 1c). The polydispersity index (PDI) values for eMIPs and eNIPs of ≈ 0.3

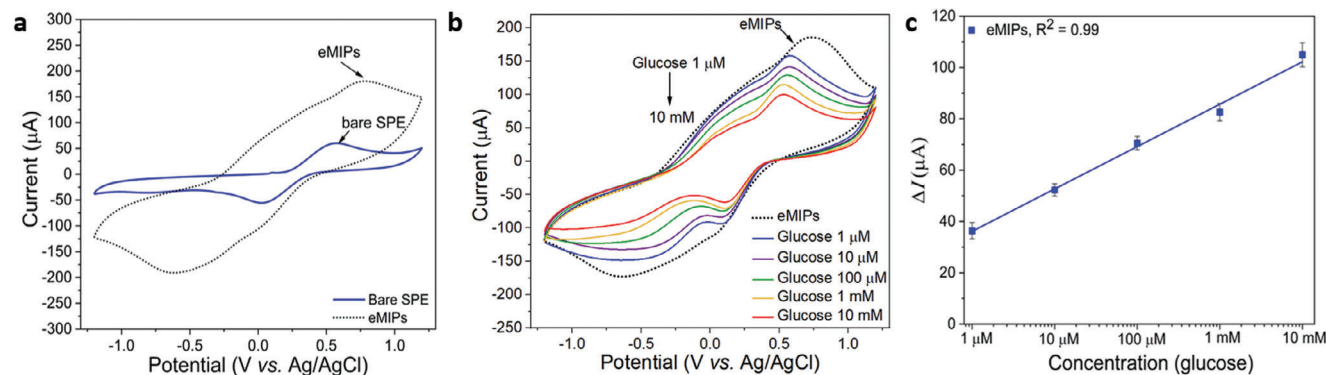


Figure 2. Cyclic voltammograms (CV) of a) bare SPE and eMIPs functionalized SPE and b) eMIPs in the presence of glucose at different concentrations in range of 1 μM–10 mM. c) Calibration curve of glucose concentration (1 μM–10 mM) on x-axis versus average change in current (ΔI) on y-axis ($n = 3$). Results are expressed as mean \pm standard deviation (SD) with error bars representing SD ($n = 3$). CV measurements were performed in 0.1 M PBS (pH 7.0) containing 0.1 M KCl and 3.0 mM $[\text{Fe}(\text{CN})_6]^{3-/4-}$ (buffer 4) at the scan rate of 50 mV s⁻¹.

demonstrated that the nanoparticles had low polydispersity and were homogenous. Homogeneous particles are particularly important as they can be distributed evenly over the electrode area to enhance the sensor's performance.^[45] TEM results revealed that eMIPs (Figure 1d) and eNIPs (Figure 1e) were spherical in shape due to the use of Pluronic P84 in the synthesis process. Pluronic P84, known for its surfactant properties, exhibits a tendency to self-assemble into spherical micelles when introduced into aqueous solutions. Consequently, it is postulated that the alignment of Py monomers with the spherical structure of Pluronic P84 micelles facilitates the formation of spherical PPy particles.^[46] The size distribution histogram constructed from TEM results showed an average particle size of 63 ± 11 nm (Figure S1a, Supporting Information) and 69 ± 16 nm (Figure S1b, Supporting Information) for eMIPs and eNIPs, respectively (Supporting Information). Additionally, TEM images of eMIPs and eNIPs were captured at higher magnification. TEM images for eMIPs are shown in Figure 1f-i,ii and for eNIPs in Figure 1f-iii,iv. Comparing the TEM images of eMIPs and eNIPs, lighter areas of lesser electron density can be observed, which are abundant throughout the nanoparticle structure of the eMIPs and might indicate the presence of imprinted cavities. Moreover, the particle sizes measured by TEM were consistently smaller than those obtained from the DLS measurements for both eMIPs and eNIPs. This disparity could be attributed to the differing physical states of the nanoparticles during the measurements. In TEM, eMIPs/eNIPs were in a dry state whereas these were in solution during DLS measurements, causing them to swell and thus increase in size. Moreover, DLS measures the D_h , which includes the hydration sphere (where water molecules surround the surface of nanoparticles) of eMIPs/eNIPs, thus larger particle size is observed compared to TEM.^[47] eMIPs-functionalized SPEs (eMIPs-SPEs) were developed by drop-casting eMIPs onto the SPEs and eMIPs-SPEs were dried at RT (25 °C) for 10 min before use (Figure 1g). Scanning electron microscopy (SEM) was used to investigate eMIP loading on the SPEs. Comparing the SEM images of the bare SPEs (Figure 1h) and eMIPs-SPEs (Figure 1i) clearly showed that eMIPs covered the full surface of SPEs, thus confirming the successful deposition of the eMIPs nanoparticles. Additionally, SEM image of different eMIPs-SPEs prepared using another batch

of eMIPs is presented in Figure S1c (Supporting Information). These results also showed similar loadings of eMIPs onto the different SPE which further demonstrated the fabrication stability of our eMIPs-SPEs via drop-casting method.

2.2. Electrochemical Measurements

CV measurements were first conducted to determine the best optimal response of the developed eMIPs-SPEs sensor. Therefore, four different buffer compositions (Electrochemical Measurement) were tested using eMIPs-SPEs. The developed sensor showed a stable response in 0.1 M PBS containing 0.1 M KCl and 3.0 mM $[\text{Fe}(\text{CN})_6]^{3-/4-}$ pH 7.0 (buffer 4), therefore, this buffer was chosen as the supporting electrolyte to perform all CV measurements. The bare SPE in buffer 4 showed an oxidation peak between +0.4 and +0.5 V for $[\text{Fe}(\text{CN})_6]^{3-/4-}$ whereas PPy based eMIPs-SPEs (prepared according to Section 2.1) showed an oxidation peak between +0.7 and +0.8 V (Figure 2a), in agreement with previous literature reports.^[48] There was no overlap between oxidation peaks of $[\text{Fe}(\text{CN})_6]^{3-/4-}$ and eMIPs, which indicated that the presence of $[\text{Fe}(\text{CN})_6]^{3-/4-}$ did not interfere or negatively impact the electrochemical sensor response. Moreover, the oxidation peak of eMIPs was also observed to be between +0.7 and +0.8 V in different buffered solutions (buffer 1–3); however, the oxidation peak was not stable since the peak current decreased with every scan in those buffers (Figure S2a–c, Supporting Information).

2.3. Electrochemical Detection of Glucose with eMIPs Sensor

eMIPs-SPEs were incubated for 5 min with 5 μL of PBS solutions containing increasing concentrations of glucose from 1 μM to 10 mM and CV measurements were recorded in buffer 4. It was observed that the oxidation peak current (I_p) decreased linearly with increasing the logarithmic concentration of glucose ($n = 3$) from 1 μM to 10 mM (Figure 2b). Similar results were observed from the CV measurements on different batches of eMIPs (Figure S2d, Supporting Information). This could be attributed to the specific recognition of glucose by the complementary binding sites present in the eMIPs. As eMIPs are porous materials,

Table 1. Comparison between eMIPs-sensor developed in this work and other glucose sensors reported in the literature.

Sensor	Detection method	Linear range (mM)	LOD (mM)	Refs.
PtE/APBA/PPy MIP	Chrono impedimetric	1–45	0.3	[38]
MIP-micelles/Au electrode	differential pulse stripping voltammetry (DPSV)	0.2–8	10	[39]
Au NPs modified MIP film	CV	10^{-6} – 10^{-4} and 10^{-4} – 1.0^{-4}	3×10^{-8}	[40]
Ferrocene modified eMIPs	DPV	0.8–50	0.43	[52]
AuNP-MIPs	SWV and EIS	1.25×10^{-6} – 0.2	1.25×10^{-6}	[54]
Fe ₃ O ₄ nanosphere/Au-GOx/MIPs	CV	0.01–5.0	0.005	[53]
MIPs/Au-SPE	CV, DPV, EIS	0.0027–0.277	0.0032	[55]
MIP/Au-electrode	SWV	0.005–0.12	0.0011	[56]
PPy/GOx/AuNPs/GRE	Amperometry	0.99–19.9	0.20	[57]
PVA/MnO ₂ @GO/CuO MIP	CV	500–4400	53	[58]
Ni-NPs/PPy/GRE	Amperometry	0.001–1	0.0004	[59]
PPy/GOx/PPy	Amperometry	0.5–24	0.026	[60]
PPy-eMIPs	CV	0.001–10	26×10^{-6}	This work

PPy: polypyrrole, GOx: glucose oxidase, PVA: polyvinyl acetate, GO: graphene oxide, APBA: aminophenylboronic acid, PtE: platinum screen-printed electrode, Ni-NPs: Nickel nanoparticles, GRE: graphite rod electrode, ITO: indium/tin oxide electrode, Au: goldAu NPs: gold nanoparticles, Au-SPE: gold screen printed electrode.

the binding of glucose to the imprinted cavities reduces the permeability of the electrode-nanoparticles interface, leading to a decrease in the current signal of the electroactive PPy as the glucose concentration increases.^[49,50] Similar results were observed by Xu et al. who also reported that the differential pulse voltammetry current for the prepared gold nanoparticles/MIPs modified indium/tin oxide (ITO) electrode decreased as the concentration of glyphosate (analyte) increased.^[51] Furthermore, the change in current (ΔI) which is the difference between the CV peak current value detected in the absence ($I_{p(eMIPs)}$) and in the presence of glucose ($I_{p(glucose)}$) at the relevant concentration was calculated (Equation 1). A calibration curve (ΔI versus Glucose concentration) was plotted by taking the average ΔI values of three experiments ($n = 3$), expressed as mean \pm standard deviation (SD). CV results observed that the ΔI increased linearly (40 ± 3 to $105 \pm 3 \mu A$) as the glucose concentration increased ($1 \mu M$ to $10 mM$) with a high correlation coefficient (R^2) of 0.99 (Figure 2c).

$$\Delta I = I_{p(eMIPs)} - I_{p(glucose, 1\mu M \text{ to } 10 mM)} \quad (1)$$

Furthermore, the LOD for the developed sensor was $\approx 26 nm$ ($LOD = 3S_b/m$) where S_b is the standard deviation of the blank signal and m is the slope of the calibration curve which suggests that the obtained biosensor exhibited an excellent specificity rivaling the reported or existing sensors (Table 1). A wide range of methods have been proposed for the electrochemical detection of glucose. However, the method used for sensor development are often labor intensive, not commercially viable, and might require surface modification with nanoparticles to enhance the electrochemical response. For instance, multiple monomers were used to synthesize nanoMIPs for electrochemical sensing of glucose, which resulted in low-yield and is not economically feasible, thereby limiting its commercial potential. Moreover, it required inclusion of ferrocene, a redox probe, which can limit overall affinity and complicate the manufacturing process.^[52] The eMIPs sensors developed in this project use a single monomer (Py) for specific binding of glucose, which reduces the overall produc-

tion cost and facilitates a scalable and straightforward manufacturing process. Other reports require surface modification of either MIPs with AuNPs or glucose oxidase enzyme (GOx) for glucose detection (LOD of $5 \mu M$), such as using of multifunctional bio-nanospheres with boric acid-derived MIPs.^[53,54] Similarly, an electropolymerized MIP deposited onto Au SPEs was used for the sensing of glucose in saliva samples of healthy volunteers and a LOD was found to be $3.2 \mu M$.^[55] A glucose imprinted MIP polymerized on the Au electrode using UV-light radiation showed a LOD $1.1 \mu M$ in a linear range of 5.0 – $120 \mu M$ with SWV.^[56] These reports have several drawbacks including tedious polymerization process, not commercially feasible due to high material or electrode cost (commercial Au electrodes are around $\pounds 250$ or $\pounds 5$ for Au SPEs); and inconsistency in MIP layer homogeneity with each polymerization. Besides that, these MIP sensors have not been tested with clinical samples of diabetic patients and therefore commercial feasibility and sensor utilization is unknown.

2.4. Specificity of eMIPs sensor

The specificity of the glucose eMIPs sensors was evaluated using eNIPs functionalized SPEs (eNIPs-SPEs). For this, the eNIPs-SPEs were incubated with solutions of PBS with different concentrations of glucose ($1 \mu M$ to $10 mM$) and only a minimal decrease in current was observed (Figure 3a). The ΔI was observed to be negligible ($\approx 13 \mu A$) at the glucose concentration of $10 mM$ on eNIPs-SPEs compared to eMIPs ($\approx 105 \mu A$) at the same glucose concentration ($n = 3$, Figure 3b). These results can be attributed to the fact that glucose-complementary imprinted sites were absent in the eNIPs sensor. Therefore, no binding of glucose on eNIPs-SPEs was observed, indicating the high specificity of the eMIPs based glucose sensor. Similar results were reported by Masoudi et al. who also observed that there was negligible binding with the eNIPs as compared to glucose imprinted CuO/MnO₂/MIPs.^[58] Furthermore, Sehit et al. utilized AuNP-MIPs modified gold electrode for the electrochemical detection

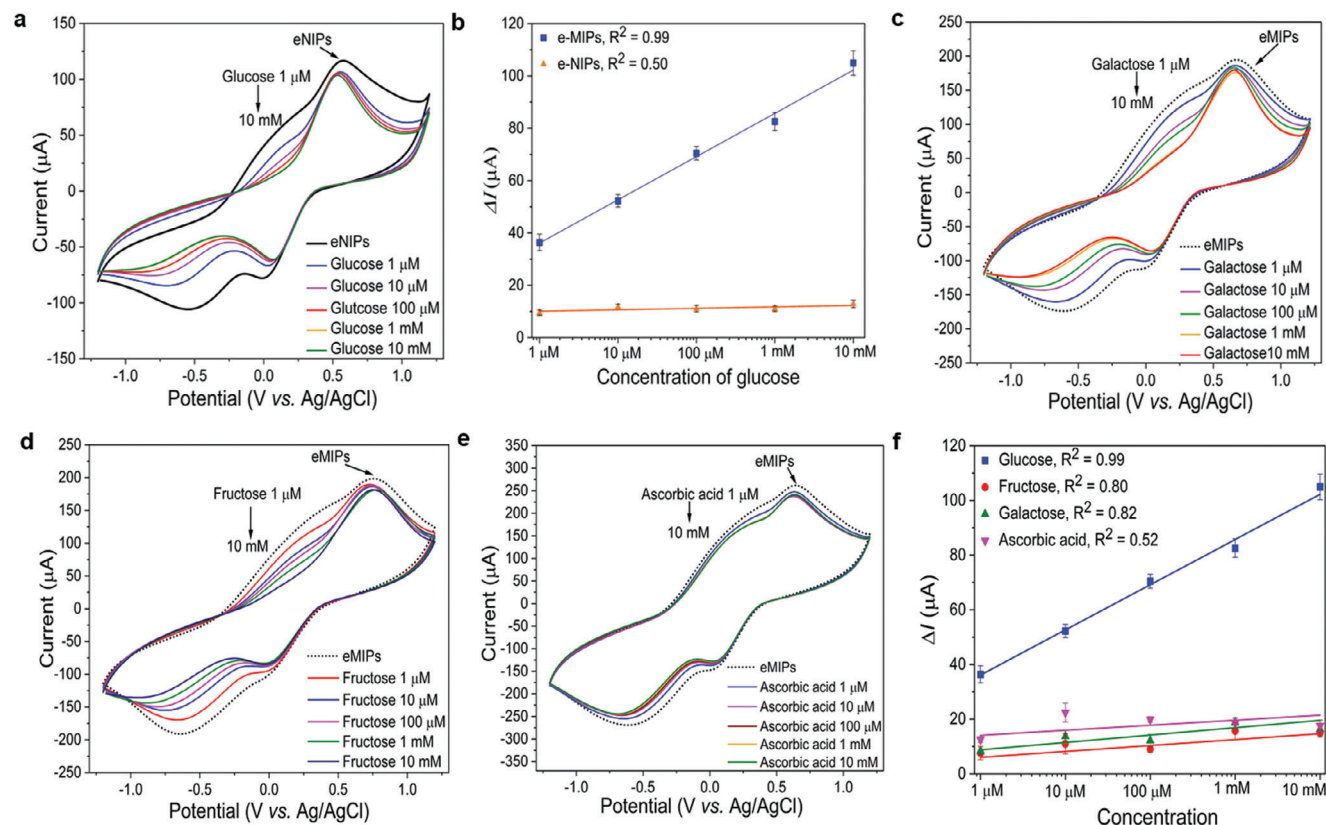


Figure 3. a) CVs of eNIPs at different glucose concentrations (1 μM –10 mM). b) Calibration curve of glucose (1 μM –10 mM) with eNIPs at x-axis versus change in current (ΔI) at y-axis. Selectivity of glucose imprinted eMIPs sensor with various interferent molecules: c) galactose, d) fructose, and e) ascorbic acid. f) Comparison of eMIPs with interferents and glucose at various concentrations (1 μM –10 mM) at x-axis versus ΔI at y-axis in buffer 4 at 50 mV s^{-1} scan rate (error bar represents SD, $n = 3$).

of glucose and the prepared sensor showed no significant change in current with glucose in the presence of eNIPs.^[54]

Imprinting factor (IF) was calculated by taking the ratio of the slope^[61] (m) of the calibration curves of eMIPs ($y = 7.273\ln(x) + 86.082$) and eNIPs ($y = 0.266\ln(x) + 11.81$) as described in Equation 2:

$$\text{IF} = m_{\text{eMIP}} / m_{\text{eNIP}} \quad (2)$$

IF was found to be ≈ 27 for our eMIPs and showed the specificity of eMIPs toward glucose, which indirectly confirm the imprinting of the glucose in the eMIPs. These results are higher or comparable to those reported for other MIP-based sensors, which typically have IF values ranging from 2 to 23.^[61–63]

2.5. Selectivity of eMIPs Sensor

Human blood has a complicated matrix that contains ample compounds such as ascorbic acid, sugars, and a mixture of proteins, which can foul the electrode surface and interfere with the sensing mechanism.^[64,65] Galactose and fructose are monosaccharides which are present in blood along with glucose and thus impact sensing.^[65,66] Ascorbic acid interference is particularly relevant because it co-exists with glucose in blood and can affect the accuracy of glucose measurements.^[67] Therefore, the

selectivity of the eMIPs sensors was assessed against possible interferents including galactose, fructose, sucrose, and ascorbic acid using the same concentration range of glucose used in this study (1 μM –10 mM). CV measurements were recorded and the change in peak current was calculated for each sample. CV results showed almost no decrease in current with the incubation of galactose, fructose, and ascorbic acid (1 μM –10 mM) to the eMIP-SPEs (Figure 3c–e). At the highest (10 mM) concentration, ΔI was measured as only ≈ 16 , ≈ 14 , and ≈ 18 μA for galactose, fructose, and ascorbic acid, respectively. These values for ΔI were significantly lower compared to the ΔI response for glucose (≈ 105 μA). This can be attributed to the incompatibility of the binding sites in the prepared eMIPs sensor with the above interferents. On the other hand, sucrose showed significant binding to the eMIPs at all the investigated concentrations. This is because sucrose is composed of 50% glucose and 50% fructose and the presence of glycosyl units in its structure is similar to glucose (Figure S2e, Supporting Information). It is worth mentioning that sucrose binding to the eMIPs sensor will not hinder glucose detection in blood samples since it is not found in human blood. High affinity for sucrose has previously been reported for glucose MIP sensor, in agreement with our observations.^[54,55] The comparative graph (ΔI versus concentration) of interferents (galactose, fructose, and ascorbic acid) and glucose with eMIPs (Figure 3f) showed that no significant change was observed with other interferents as

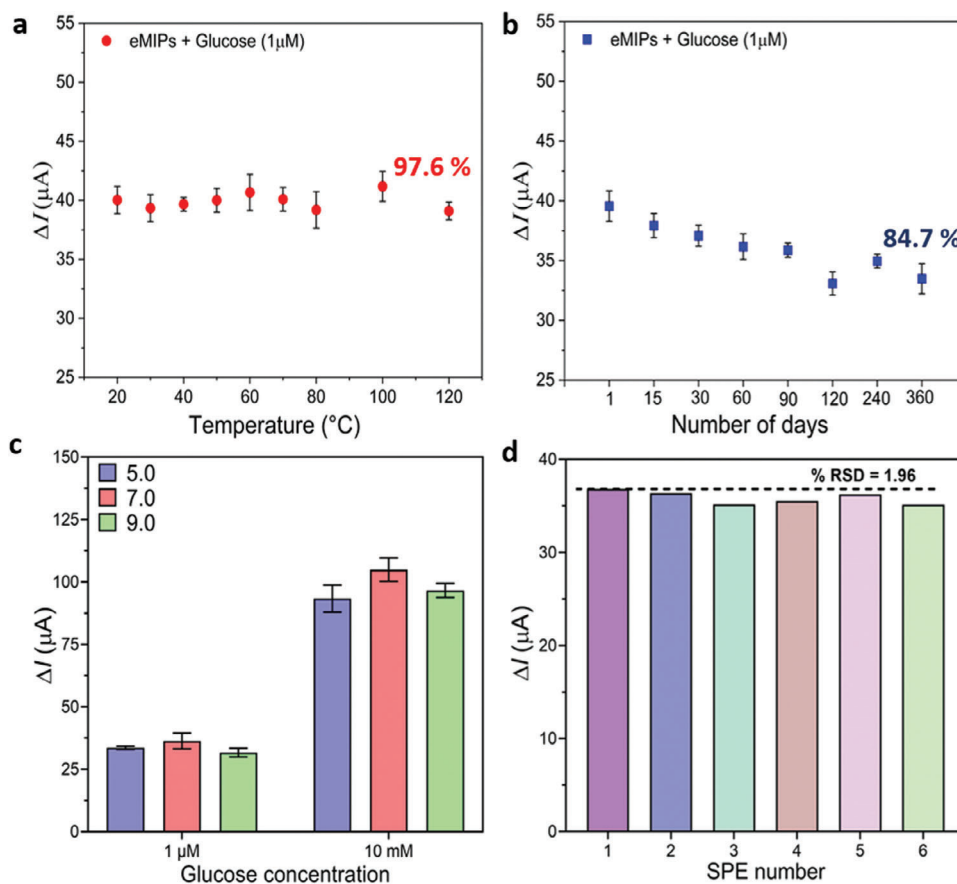


Figure 4. a) Robustness of eMIPs sensor when exposed to temperatures of 20–120 °C for 30 min. b) Long-term stability study of eMIPs sensor on different days (1–360 days). The eMIPs sensor was tested in a 1 μM glucose concentration in PBS. c) Effect of different pH (5.0, 7.0, and 9.0) on the stability of eMIPs sensor when incubated with glucose at two different concentrations (1 μM and 10 mM). d) Reproducibility study of eMIPs-SPEs sensor ($n = 6$) in the presence of 1 μM glucose. Experiments were performed in triplicates ($n = 3$). Error bars represent SD.

compared to glucose. These observations highlight the high selectivity of eMIPs sensors toward glucose.

2.6. Robustness, Stability and Reproducibility

The robustness of the eMIPs sensor was evaluated by measuring its ΔI response with glucose concentration (1 μM) over various temperatures ranging from 20 to 120 °C. Moreover, the stability of eMIPs was determined over a one-year time (1 to 360 days). The eMIPs sensor retained 98% of its original sensor response after incubation at 120 °C (Figure 4a) and 85% after 360 days (Figure 4b), respectively. Our results were well corroborated with literature reports. For instance, Sehit et al. assessed the stability of gold nanoparticles-based eMIP sensor over a 40-day period, revealing a slight signal decrease. Diouf et al. also observed the stability of eMIP based glucose sensor for a period of 3 months, with the sensor preserving 85% of its initial response.^[54,55] In contrast, our developed sensor demonstrated a very high stability over one year, retaining 85% of the initial response. These results show that our eMIPs sensor is highly robust and stable, even under extreme conditions whereas enzyme-based glucose sensors are only stable at low tempera-

tures (4 °C). The pH value has a significant role in the electrochemical reaction between the analyte and electrode.^[68] Therefore, buffered solutions consisting of 0.1 M PBS, $[Fe(CN)_6]^{3-/4-}$ and 0.1 M KCl with different pH values (i.e., pH 5.0, 7.0, and 9.0) were used to observe the effect of pH on binding of glucose to the eMIPs. It was observed that eMIPs incubation with glucose (at 1 μM and 10 mM respectively) showed slightly higher ΔI responses at the physiological pH 7.0 compared to pH 5.0 and 9.0, indicating that glucose had higher interactions with imprinted cavities at pH 7.0 (Figure 4c). However, pH did not affect the sensing performance significantly and the changes in ΔI response was statistically negligible which further confirmed the stability and robustness of our eMIPs sensor.^[69] The developed eMIPs sensor provide a more reliable and practical glucose sensing compared to common enzyme-based sensors that suffer from instability issues as the activity of enzymes (like GOx) can be easily influenced by temperature and buffer pH.^[70] Furthermore, to evaluate the reproducibility of eMIPs-SPE sensors, the electrochemical behavior of six different eMIPs-SPEs ($n = 6$), prepared in two batches (3 SPEs per batch of eMIPs) under identical conditions and the same amount of eMIPs nanoparticles, was studied using CV. The ΔI response of different SPEs incubated with 1 μM of glucose (Figure 4d)

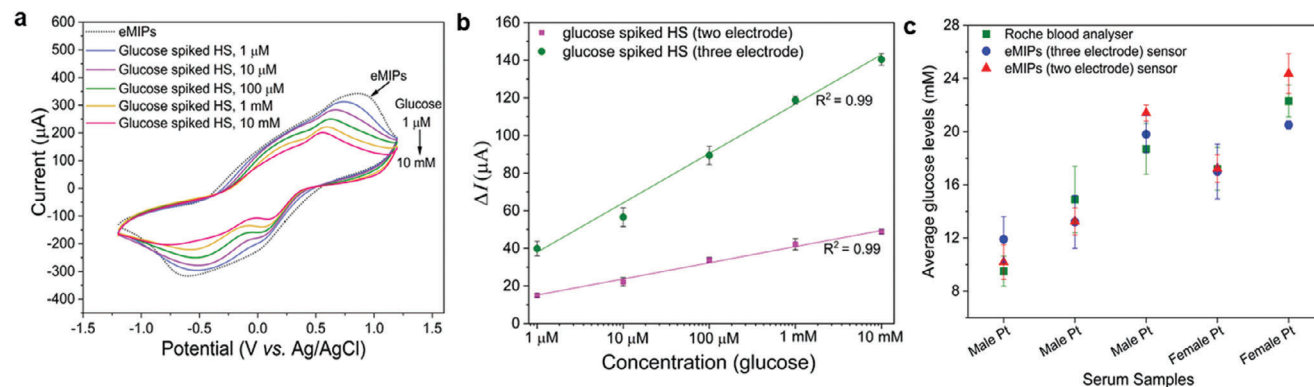


Figure 5. a) CVs of eMIPs with glucose (1 μM –10 mM) spiked human serum (HS, 100X diluted) in a three-electrode setup. b) Calibration curves of glucose concentration in HS (1 μM –10 mM) versus ΔI in three-electrode and two-electrode setups ($n = 3$). c) Comparison of average glucose levels in five different (male and female) diabetic patients' (Pt) serum samples determined using Roche blood analyzer (hospital method) and eMIPs sensor in three-electrode and two-electrode setups. Error bars represent SD.

showed similar values across all SPEs, with a relative standard deviation (RSD) of 1.96%, indicating the high reproducibility of the eMIPs-SPE sensors. Similar observations were reported previously on PPy-based eMIPs for the electrochemical detection of *Klebsiella pneumoniae* (RSD of 1.8%)^[37] and on metal-organic framework based PPy-eMIPs for the determination of dopamine in human serum samples (RSD of 2.25%).^[71] The prepared sensor exhibited consistent performance, showcasing its ability to maintain a reliable and reproducible response over time. This robust and long-term stable behavior underscores the durability and long-term effectiveness of the eMIPs sensor, enhancing its potential for practical applications in various sensing scenarios.

2.7. Electrochemical Detection of Glucose with a Two-Electrode Setup

As a proof of concept, CV measurements were also carried out with a two-electrode setup using eMIPs-SPE as WE and Pt wire as CE. CV results revealed that the incubation of glucose (1 μM –10 mM) with eMIPs sensor had a concentration dependent decrease in current (Figure S3a, Supporting Information). The calibration curve of ΔI versus glucose concentrations (1 μM –10 mM) showed a linear relationship as depicted in Figure S3b (Supporting Information). There was no significant difference in the CV results obtained from the two-electrode and three-electrode setups (Section 3.3) and there was a high correlation (0.98) between the data. Compared to the conventional three-electrode systems commonly used for biosensing, the two-electrode setup could be easier and cheaper to make and is more commercially viable since it does not rely on the use of a reference electrode which can be expensive. Additionally, the two-electrode systems eliminate the need for complicated measurement setups as they may be easily used in conjunction with traditional electronics and therefore have relevance toward developing miniaturized wearable sensors. The high correlation of the sensing response between the two-electrode and three-electrode systems opens doors to developing wearable sensors that are tiny, easy to fabricate, scalable, and cost-effective.

2.8. Electrochemical Detection of Glucose in Real Samples

2.8.1. Detection of Glucose in Spiked Human Serum Samples

The nonspecific adsorption of numerous biomolecules present in complex sample matrix (serum, blood/plasma, and saliva) can lead to fouling at the electrode interface. This can significantly impede electrochemical performance, a reduction in both the sensitivity and specificity of the biosensor's electrochemical signal.^[72] However, our developed sensor was able to detect glucose concentrations (1 μM –10 mM) with high sensitivity ($\approx 2.91 \mu\text{A}$ and $0.608 \mu\text{A} \mu\text{M}^{-1} \text{mm}^{-2}$), in spiked human serum (HS) samples using both three-electrode (Figure 5a) and two-electrode systems (Figure S3c, Supporting Information) respectively. The calibration curve for the three-electrode and two-electrode sensors showed linear relationships between ΔI and logarithmic glucose concentration (mM) with a high correlation coefficient (R^2) of 0.99 (Figure 5b). However, the difference in the ΔI of two and three electrode system can be attributed to the fact that in a two-electrode system, the counter electrode is actually utilized as the reference electrode. Unlike the dedicated reference electrode, the potential of the counter electrode fluctuates during measurement, leading to varying results. Many literature studies have reported the glucose sensing in diluted HS using non-enzymatic electrochemical sensors but those typically require alkaline media.^[73,74] Our study achieved the glucose detection in the physiological pH range without the need for an expensive and time-consuming preparation process.

2.8.2. Detection of Glucose in Diabetic Patients' Serum Samples

A random venous blood (serum) glucose level $\geq 11 \text{ mM}$ or a fasting blood glucose level $\geq 7 \text{ mM}$ on two or more separate occasions, is indicative of a probable diagnosis of diabetes in an individual.^[75,76] Therefore, the real time applicability, reliability, and accuracy of the proposed eMIPs sensors were investigated to determine glucose in serum samples of diabetic patients. The samples from five different patients (Pt.) including males and females with old DM histories were tested to measure

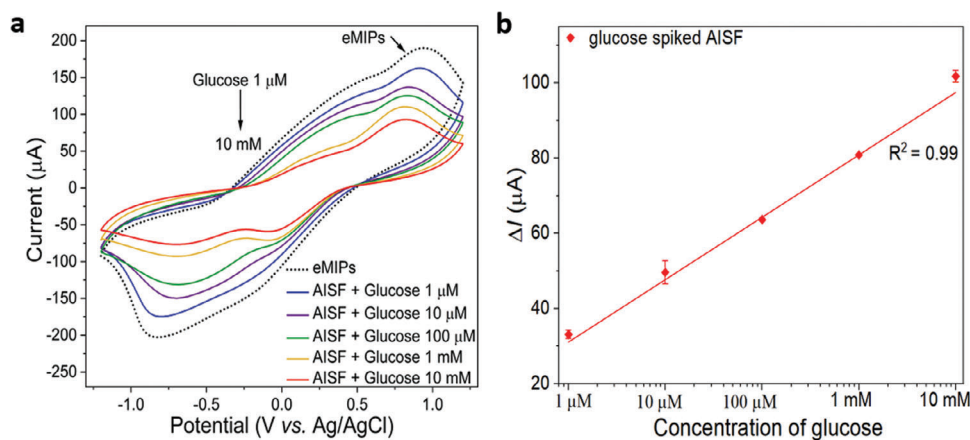


Figure 6. a) CVs of eMIPs with glucose (1 μM –10 mM) spiked artificial interstitial fluid (AISF). b) Calibration curves of ΔI versus glucose concentration (1 μM –10 mM) in AISF (pH 7.4) in three-electrode electrode setup ($n = 3$). Error bars represent SD.

glucose levels. The glucose concentration (mM) obtained with eMIPs sensor (in both three-electrode and two-electrode setups) showed no significant difference (confidence coefficient 95%) compared to the Roche blood analyzer results (data from Newcastle upon Tyne Hospital Trust). The concentration of glucose in the diabetic serum samples was determined using a calibration curve of glucose spiked HS (for both three-electrode and two-electrode systems) and the results (in triplicates) were presented in Figure 5c. The correlation coefficients for the three-electrode and two-electrode systems with the Roche blood analyzer (hospital method) was found to be 0.93 and 0.96, respectively. Correlation coefficients with magnitudes between 0.9 and 1.0 indicate very high levels of correlation between variables. Thus, these findings demonstrated a significant correlation between the prepared sensors and the established hospital method/Roche blood analyzer, affirming the reliability of the developed eMIPs-based electrochemical sensor. Notably, the correlation between the results obtained from the two-electrode and three-electrode setups further underscores the robustness of the developed material and sensor platform. These results collectively support the practical application of the prepared sensors in real-time glucose detection.

2.8.3. Application of eMIPs Sensor in Artificial Interstitial Fluids

Wearable monitoring for glucose can be carried out in ISF (the liquid just below the skin) because ISF is very similar in composition to plasma/serum and can be extracted using non-invasive methods such as reverse iontophoresis and hydrogel microneedle patches.^[77,78] Since glucose freely diffuses from capillaries into the interstitial space, the glucose level in the ISF is a reliable indicator of the blood glucose level.^[79] Understanding the behavior of glucose in an environment similar to ISF could provide a reliable and practical understanding of the real-life performance of the sensor for diabetes management practices.^[80,81] We validated the performance of the eMIPs sensor in glucose (1 μM to 10 mM) spiked artificial ISF (AISF, pH 7.4). Monitoring the current response revealed a concentration dependent decrease in the peak current (Figure 6a). Furthermore, the calibration curve of

ΔI versus glucose spiked AISF (1 μM to 10 mM) concentrations (in logarithmic scale) showed a linear relationship (Figure 6b) with a R^2 of 0.99 ($n = 3$) and a LOD of 44 nM. Notably, a similar trend for ΔI response was observed with AISF samples as with ΔI response for the three-electrode system and spiked HS samples. The ability of eMIPs sensor to determine the glucose levels in AISF samples (1 μM to 10 mM) and a strong correlation with results from spiked serum samples (≈ 0.99) suggest the suitability of our eMIPs sensor for the development of wearable sensors.

3. Conclusion

This is the first report which demonstrate a novel method for the fabrication of PPy based eMIPs sensor for the monitoring of glucose in real samples of diabetic patients. The production of eMIPs involves a straightforward, cost-effective, and facile bulk synthesis process that eliminates the need for lengthy and expensive fabrication steps and materials such as enzymes, AuNPs, and carbon dots. The developed sensor is inexpensive (SPEs < \$0.1) and has high robustness (withstanding 120 °C), long-term stability (12 months), fast response time (< 30 s), excellent selectivity, and specificity. CV measurements revealed highly specific binding of glucose with eMIPs based sensor in a wide working range (1 μM –10 mM) with a LOD of ≈ 26 nM (or ≈ 136 nM) and sensitivity of ≈ 2.91 $\mu\text{A } \mu\text{M}^{-1} \text{ mm}^{-2}$ (or ≈ 0.608 $\mu\text{A } \mu\text{M}^{-1} \text{ mm}^{-2}$) when used in a three-electrode (or two-electrode) setup. The clinical potential of the eMIPs sensor as a reliable tool for monitoring glucose levels in diabetic patients was demonstrated by showing a strong correlation (> 0.9) of the sensing signal with the data from the common Roche blood analyser. Our eMIPs sensor demonstrated a wide detection range of 1 μM to 10 mM in AISF with a LOD of ≈ 44 nM and strong correlation with serum glucose, highlighting its potential application for non-invasive measurements with wearable technology. Additionally, the use of a two-electrode setup eliminates the need for a reference electrode, enhances the versatility of the sensor, and makes it possible to achieve sensors that are easier and more cost-effective to manufacture. Given the versatility of eMIPs, this technology can extend to detecting other biological molecules like uric acid, dopamine, and

creatinine. Utilizing dual/triple SPEs enables the simultaneous detection of two or three biological molecules, critical for diabetes patients who have associated co-morbidities that need to be monitored at the same time.

4. Experimental Section

Materials: Pyrrole (Py), iron (III) chloride hexahydrate, D-glucose, fructose, galactose, sucrose, potassium ferricyanide (III), potassium hexacyanoferrate (II) trihydrate, and human serum (HS) were purchased from Sigma-Aldrich (UK). Pluronic P84 (MW = 4200 g mol⁻¹) was provided as a gift sample by BASF (Germany). Potassium chloride, Oxoid phosphate buffered saline (PBS) tablets and methanol were purchased from Fisher Scientific (UK). The serum samples from five different diabetic patients were obtained from the NovoPath Biobank (ethical approval number is 22/NE/0054, project ID is 314763) Newcastle upon Tyne Hospital Trust (UK). All chemicals and solvents used were high-performance liquid chromatography (HPLC) or analytical grade and were used without any further purification. PBS solutions were prepared with deionized (DI) water with a resistivity of ≥ 18.2 M Ω cm. All other chemicals used for the AISF preparation were of analytical grade and were procured from Sigma-Aldrich (UK).

The graphite SPEs with a diameter of ≈ 3.1 mm were made in-house using a screen-printing machine (DEK microDEK 1760RS, UK) and a suitable stencil design. First, a carbon-graphite ink (Gwent Electronic Materials Ltd, UK) was printed on a 250 μ m thick polyester substrate (Autostat). The ink was then cured at 60 °C for 30 min in an oven. Afterward, a dielectric paste (Gwent Electronic Materials Ltd, UK) was applied to cover the connections, and then cured again at 60 °C for 30 min. The resulting electrodes has a high reproducibility by showing a relative standard deviation (RSD) of less than 4.2% when tested with [Ru(NH₃)₆]^{2+/3+}/0.1 M KCl and had an average connection length of 32 mm with a working electrode resistance of 2.16 ± 0.06 k Ω . The rectangular shape of the electrodes was defined by the dielectric material, making them easy to handle.^[42]

Methods—Synthesis of eMIPs and eNIPs: D-glucose imprinted eMIPs nanoparticles were synthesized through the chemical polymerization of Py using Iron (III) chloride hexahydrate (FeCl₃·6H₂O), where Py and glucose served as the electroactive monomer and template, respectively.^[42] First, Pluronic P84 (2.3 g) and glucose (0.1 M) were dissolved in DI water (230 mL) and the mixture was stirred for 3 h at 40 °C. Py (0.1 M) was then added to the mixture and stirred for 1 h at 20 °C. Subsequently, FeCl₃·6H₂O (0.3 M) was added and the mixture was kept stirring for additional 6 h at 20 °C. The obtained eMIPs nanoparticles were then washed three times with a 50:50 mixture of methanol and water to remove any Pluronic P84 residue. In the next step, glucose (template) and unreacted monomer were removed from the eMIPs solution through refluxing with a 50:50 mixture of methanol and water (3X). Finally, glucose imprinted eMIPs were collected by filtering the solution through a sintered funnel and drying overnight at 60 °C under vacuum. eNIPs were produced using the same process without the addition of glucose and served as a reference material.

Particle Size and Morphology Characterization of eMIPs and eNIPs: The obtained eMIPs powder was subjected to Fourier transform infrared (FTIR) analysis using an attenuated total reflection (ATR)-FTIR spectrometer (Perkin Elmer UATR Spectrum Two, UK). FTIR spectra were recorded to identify the formation of the PPY polymeric material, and the functional groups present in the polymer network. Dynamic light scattering (DLS) experiments were conducted to measure the hydrodynamic diameter (D_h) of eMIPs and eNIPs using a Malvern Zetasizer Nano ZS with a 173° scattering angle and a 632.8 nm laser wavelength. Each sample was tested at different time points to check the stability of the measurements at 25 °C and all the experiments were performed in triplicate. For the morphology and particle size determination, transmission electron microscopy (TEM) measurements were performed using Hitachi HT7800 120 kV TEM machine (Japan). Briefly, a 2 mg mL⁻¹ solution of eMIPs and eNIPs in PBS (pH 7.0) was sonicated using RS pro ultrasonicator (at a frequency of 40 kHz with an ultrasonic power rating of 70 W) for 1 min and subsequently applied to a copper grid using drop-casting. To prepare the eMIPs functionalized SPEs, eMIPs solution (2 mg mL⁻¹ in PBS) was drop-cast

onto the SPEs, and eMIPs-SPEs were kept for drying at RT (25 °C) for 10 min. The morphology of the bare and eMIPs-SPEs was studied using SEM (Carl Zeiss Sigma VP FEG-SEM, Germany).

Electrochemical Measurements: Cyclic voltammetry (CV) measurements were carried out with a PalmSens4 potentiostat (PalmSens, the Netherlands) using custom-made SPEs as working electrode (WE), Ag/AgCl as reference electrode (RE), and a platinum wire (Pt) as a counter electrode (CE) at the potential range of -1.2 to $+1.2$ V (vs Ag/AgCl) and a fixed scan rate of 50 mV s⁻¹. 20 μ L of eMIPs solution (2 mg mL⁻¹ in PBS, pH 7.0) was drop cast onto SPEs and dried for 10 min at RT (25 °C), with the resulting SPEs referred to as eMIPs-SPEs. Four different buffered solutions were employed: buffer 1 (0.1 M PBS, pH 7.0), buffer 2 (0.1 M PBS, 0.1 M KCl, pH 7.0), buffer 3 (10 mM PBS, 0.1 M Na₂SO₄, pH 7.0), and buffer 4 (0.1 M PBS containing 0.1 M KCl and 3.0 mM [Fe(CN)₆]^{3-/4-} pH 7.0) to determine the optimal response of eMIPs-SPEs through CV measurements. eMIPs-SPEs were washed with DI water and incubated with 1 μ M to 10 mM concentration of glucose (in PBS, pH 7.0) for 5 min prior to the CV measurements. The calibration curve was obtained by plotting different concentrations of glucose (1 μ M to 10 mM) on the x-axis versus changes in current (ΔI) on the y-axis. Selectivity studies have also been performed using different interferents such as galactose (Gal), fructose (Fru), sucrose (Suc), and ascorbic acid (AA) at different concentrations (1 μ M–10 mM, PBS, pH 7.0). eNIPs functionalized SPEs were used to evaluate the specificity of eMIPs-SPEs sensors. CV measurements were also performed in a two-electrode set up constructed by using the same WE and CE used in the three-electrode system to further explore the potential of the prepared sensor for real-time monitoring of glucose in a wearable device.

Robustness, Stability, and Reproducibility Studies: eMIPs-SPEs were kept at different temperatures (20–120 °C) in a temperature-controlled oven for 30 min after which CV measurements were performed. For stability studies, the same batch of eMIPs was used to produce eMIPs-SPEs and tested at different time intervals over a period of one year (1st, 15th, 30th, 60th, 120th, 240th, 360th day). The capability of the eMIPs sensor to withstand various pH values (i.e., pH 5.0, 7.0, and 9.0) was investigated at minimum and maximum glucose concentrations (1 μ M and 10 mM). All the experiments were performed in triplicates (n = 3). Additionally, to determine the reproducibility of the developed sensor, six different eMIPs-SPEs were prepared from two different batches of eMIPs (3 SPEs per batch of eMIPs) prepared under the same conditions by drop-casting an equal amount of eMIPs nanoparticles onto the SPEs. CV measurements were then performed with the eMIPs-SPEs incubated with 1 μ M concentration of glucose and the relative standard deviation (RSD) in percentage was calculated.

Application of eMIPs sensors in Glucose Spiked Human Serum Samples and Serum Samples of Diabetic Patients: Glucose spiked human serum (HS) samples were prepared by mixing different concentrations of glucose (1 μ M–10 mM) with 100X diluted HS. CV measurements were performed to construct a calibration curve using eMIPs sensors. Furthermore, real serum samples from five different diabetic patients (100X diluted) were obtained from the NovoPath Biobank (ethical approval number is 22/NE/0054, project ID is 314763) and analyzed using eMIPs sensor. The concentration of glucose in the diabetic serum samples was determined using the calibration curve constructed by plotting glucose concentrations (1 μ M to 10 mM) on the x-axis versus ΔI for glucose spiked HS on the y-axis.

Application of eMIPs Sensors in Glucose Spiked AISF Solutions: To prepare the AISF, 2.5 mM CaCl₂, 10 mM HEPES (2-[4-(2-hydroxyethyl)piperazin-1-yl]ethanesulfonic acid), 3.5 mM KCl, 0.7 mM MgSO₄, 123 mM NaCl, 1.5 mM NaH₂PO₄, 7.4 mM saccharose (sucrose) were mixed, and the pH of the solution was adjusted to pH 7.4.^[68] All solutions were prepared with DI water with a resistivity of ≥ 18.2 M Ω cm.

Supporting Information

Supporting Information is available from the Wiley Online Library or from the author.

Acknowledgements

The authors would like to thank Northern Accelerator grant (grant number NACCF248) for funding this project and the industrial collaborator Mr Tommy Lovell for his active engagement and valuable discussion to deploy this technology as wearable sensors. The authors would also like to thank NovoPath Biobank, Newcastle (UK) for providing the patient samples. The authors would like to acknowledge Dr Teruo Hashimoto (Department of Materials, UoM) for conducting some of TEM experiments and for his valuable discussions. Saweta Garg expresses gratitude for the partial salary support provided by the MRC research grant (ARIA: MR/Y008421/1).

Conflict of Interest

The authors declare no conflict of interest.

Data Availability Statement

The data that support the findings of this study are available in the supplementary material of this article.

Keywords

biosensors, conductive polymers, electroactive molecularly imprinted polymer nanoparticles (eMIPs), electrochemical sensors, glucose, polypyrrole (PPy), screen printed electrodes (SPEs)

Received: April 24, 2024

Revised: July 22, 2024

Published online:

- [1] N. V. Bhilare, R. Shedge, P. M. Tambe, A. More, *Med. Chem. Res.* **2024**, *33*, 337.
- [2] T. I. D. F. (IDF) Diabetes Facts & figures, <https://idf.org/about-diabetes/diabetes-facts-figures> (accessed: February 2024).
- [3] H. Sun, P. Saedi, S. Karuranga, M. Pinkepank, K. Ogurtsova, B. B. Duncan, C. Stein, A. Basit, J. C. Chan, J. C. Mbanya, *Diabetes Res. Clin. Pract.* **2022**, *183*, 109119.
- [4] F. Picconi, M. Parravano, D. Ylli, P. Pasqualetti, S. Coluzzi, I. Giordani, I. Malandrucchio, D. Lauro, F. Scarinci, P. Giorno, *Acta Diabetologica* **2017**, *54*, 489.
- [5] J. L. Harding, M. E. Pavkov, D. J. Magliano, J. E. Shaw, E. W. Gregg, *Diabetologia* **2019**, *62*, 3.
- [6] J. Xue, C. Han, Y. Yang, S. Xu, Q. Li, H. Nie, J. Qian, Z. Yang, *Inorg. Chem.* **2023**, *62*, 3288.
- [7] A. K. M., R. Krishnamoorthy, S. Gogula, B. S. S. Muthu, G. Chellamuthu, K. Subramaniam, *Sci. Rep.* **2024**, *14*, 6151.
- [8] G. M. I. Inc, Self-monitoring Blood Glucose), By Technology (Electrochemical Biosensors, Optical Biosensors), By End-Use (Hospitals, Home Care, Diagnostic Centers & Clinics), Global Forecast, 2023–2032, <https://www.gminsights.com/industry-analysis/glucose-biosensors-market> (accessed: February 2024).
- [9] L. Olansky, L. Kennedy, *Am Diabetes Assoc.* **2010**, *33*, 948.
- [10] S. E. Inzucchi, *N. Engl. J. Med.* **2012**, *367*, 542.
- [11] R. Wilson, A. Turner, *Biosens. Bioelectron.* **1992**, *7*, 165.
- [12] Y. Li, Y.-Y. Song, C. Yang, X.-H. Xia, *Electrochem. Commun.* **2007**, *9*, 981.
- [13] S. Park, H. Boo, T. D. Chung, *Anal. Chim. Acta* **2006**, *556*, 46.
- [14] W. Gao, H. Ota, D. Kiriya, K. Takei, A. Javey, *Acc. Chem. Res.* **2019**, *52*, 523.
- [15] J. Luo, S. Jiang, H. Zhang, J. Jiang, X. Liu, *Anal. Chim. Acta* **2012**, *709*, 47.
- [16] M. Adeel, M. M. Rahman, I. Caligiuri, V. Canzonieri, F. Rizzolio, S. Daniele, *Biosens. Bioelectron.* **2020**, *165*, 112331.
- [17] M. H. Hassan, C. Vyas, B. Grieve, P. Bartolo, *Sensors* **2021**, *21*, 4672.
- [18] T. Chang, H. Li, N. Zhang, X. Jiang, X. Yu, Q. Yang, Z. Jin, H. Meng, L. Chang, *Microsyst. Nanoeng.* **2022**, *8*, 25.
- [19] J. Hanna, Y. Tawk, S. Azar, A. H. Ramadan, B. Dia, E. Shamieh, S. Zoghbi, R. Kanj, J. Costantine, A. A. Eid, *Sci. Rep.* **2022**, *12*, 14885.
- [20] H. Lee, Y. J. Hong, S. Baik, T. Hyeon, D. H. Kim, *Adv. Healthcare Mater.* **2018**, *7*, 1701150.
- [21] S. R. Corrie, J. Coffey, J. Islam, K. Markey, M. Kendall, *Analyst* **2015**, *140*, 4350.
- [22] Y. C. Kudva, A. J. Ahmann, R. M. Bergenstal, J. R. Gavin III, D. F. Kruger, L. K. Midyett, E. Miller, D. R. Harris, *J. Endocr. Soc.* **2018**, *2*, 1320.
- [23] R. A. Ajjan, M. H. Cummings, P. Jennings, L. Leelarathna, G. Rayman, E. G. Wilmot, *Diabetes Vasc. Dis. Res.* **2018**, *15*, 175.
- [24] Healthline Comparing Top Glucose Monitoring Devices, <https://www.healthline.com/diabetismine/dexcom-vs-abbott-freestyle-libre-cgm-function-accuracy-and-cost> (accessed: March 2024).
- [25] S. Alexander, P. Baraneedharan, S. Balasubrahmanyam, S. Ramaprabhu, *Eur. Polym. J.* **2017**, *86*, 106.
- [26] S. A. Piletsky, A. P. Turner, *Electroanalysis* **2002**, *14*, 317.
- [27] Z. Zeng, Y. Hoshino, A. Rodriguez, H. Yoo, K. J. Shea, *ACS Nano* **2010**, *4*, 199.
- [28] F. Canfarotta, J. Czulak, A. Guerreiro, A. G. Cruz, S. Piletsky, G. E. Bergdahl, M. Hedström, B. Mattiasson, *Biosens. Bioelectron.* **2018**, *120*, 108.
- [29] B. V. Silva, B. A. Rodríguez, G. F. Sales, T. S. Maria Del Pilar, R. F. Dutra, *Biosens. Bioelectron.* **2016**, *77*, 978.
- [30] Z. Chen, C. Wright, O. Dincel, T.-Y. Chi, J. Kameoka, *Sensors* **2020**, *20*, 1098.
- [31] M. d. L. Gonçalves, L. A. Truta, M. G. F. Sales, F. T. Moreira, *Anal. Lett.* **2021**, *54*, 2611.
- [32] H. Chen, M. B. Müller, K. J. Gilmore, G. G. Wallace, D. Li, *Adv. Mater.* **2008**, *20*, 3557.
- [33] S. Ramanavičius, I. Morkvėnaitė-Vilkonienė, U. Samukaitė-Bubnienė, V. Ratautaitė, I. Plikusienė, R. Viter, A. Ramanavičius, *Sensors* **2022**, *22*, 1282.
- [34] M. Omastová, S. Kosina, J. Pionteck, A. Janke, J. Pavlinec, *Synth. Met.* **1996**, *81*, 49.
- [35] M. A. Alonso-Lomillo, O. Domínguez-Renedo, *Talanta* **2023**, *253*, 123936.
- [36] V. Ratautaitė, R. Boguzaitė, E. Brazys, A. Ramanaviciene, E. Ciplys, M. Juozapaitis, R. Slibinskas, M. Bechelany, A. Ramanavicius, *Electrochim. Acta* **2022**, *403*, 139581.
- [37] R. Sharma, G. Lakshmi, A. Kumar, P. Solanki, *ECS Sensors Plus* **2022**, *1*, 010603.
- [38] Z. Onur Uygun, H. D. Ertuğrul Uygun, *Electroanalysis* **2020**, *32*, 226.
- [39] Y. Yang, C. Yi, J. Luo, R. Liu, J. Liu, J. Jiang, X. Liu, *Biosens. Bioelectron.* **2011**, *26*, 2607.
- [40] W. Zhao, R. Zhang, S. Xu, J. Cai, X. Zhu, Y. Zhu, W. Wei, X. Liu, J. Luo, *Biosens. Bioelectron.* **2018**, *100*, 497.
- [41] J. McClements, L. Bar, P. Singla, F. Canfarotta, A. Thomson, J. Czulak, R. E. Johnson, R. D. Crapnell, C. E. Banks, B. Payne, *ACS Sens.* **2022**, *7*, 1122.
- [42] R. D. Crapnell, R. J. Street, V. Ferreira-Silva, M. P. Down, M. Peeters, C. E. Banks, *Anal. Chem.* **2021**, *93*, 13235.
- [43] E. Sehit, Z. Altintas, *Biosens. Bioelectron.* **2020**, *159*, 112165.
- [44] A. Umer, F. Liaqat, A. Mahmood, *Polymers* **2020**, *12*, 353.
- [45] P. Singla, G. Parokie, S. Garg, S. Kaur, I. Kaur, R. D. Crapnell, C. E. Banks, U. Rinner, C. Wills, M. Peeters, *J. Drug Deliv. Sci. Technol.* **2023**, *83*, 104403.

- [46] P. Singla, O. Singh, S. Sharma, K. Betlem, V. Aswal, M. Peeters, R. Mahajan, *ACS Omega* **2019**, *4*, 11251.
- [47] P. Singla, S. Kaur, O. Jamieson, A. Dann, S. Garg, C. Mahon, R. D. Crapnell, C. E. Banks, I. Kaur, M. Peeters, *Anal. Bioanal. Chem.* **2023**, *415*, 4467.
- [48] M. Bharath, A. T. Mathew, K. Akshaya, U. Sirimahachai, A. Varghese, G. Hegde, *RSC Adv.* **2022**, *12*, 17036.
- [49] S. Ding, Z. Lyu, S. Li, X. Ruan, M. Fei, Y. Zhou, X. Niu, W. Zhu, D. Du, Y. Lin, *Biosens. Bioelectron.* **2021**, *191*, 113434.
- [50] H. E. Sharif, S. R. Dennison, M. Tully, S. Crossley, W. Mwangi, D. Bailey, S. Graham, S. Reddy, *Anal. Chim. Acta* **2022**, *1206*, 339777.
- [51] J. Xu, Y. Zhang, K. Wu, L. Zhang, S. Ge, J. Yu, *Microchim. Acta* **2017**, *184*, 1959.
- [52] A. Garcia-Cruz, O. Ahmad, K. Alanazi, E. Piletska, S. Piletsky, *Microsyst. Nanoeng.* **2020**, *6*, 83.
- [53] Y. Cheng, T. Chen, D. Fu, M. Liu, Z. Cheng, Y. Hua, J. Liu, *Talanta* **2022**, *242*, 123279.
- [54] E. Sehit, J. Drzazgowska, D. Buchenau, C. Yesildag, M. Lensen, Z. Altintas, *Biosens. Bioelectron.* **2020**, *165*, 112432.
- [55] A. Diouf, B. Bouchikhi, N. El Bari, *Mater. Sci. Eng. C.* **2019**, *98*, 1196.
- [56] C. Fang, C. Yi, Y. Wang, Y. Cao, X. Liu, *Biosens. Bioelectron.* **2009**, *24*, 3164.
- [57] N. German, A. Ramanavicius, A. Ramanaviciene, *Electroanalysis* **2017**, *29*, 1267.
- [58] M. M. Farid, L. Goudini, F. Piri, A. Zamani, F. Saadati, *Food Chem.* **2016**, *194*, 61.
- [59] G. Emir, Y. Dilgin, A. Ramanaviciene, A. Ramanavicius, *Microchem. J.* **2021**, *161*, 105751.
- [60] J. G. Ayenimo, S. B. Adeloju, *Food Chem.* **2017**, *229*, 127.
- [61] F. Gagliani, T. Di Giulio, S. Grecchi, T. Benincori, S. Arnaboldi, C. Malitesta, E. Mazzotta, *Molecules* **2024**, *29*, 1632.
- [62] J. Huang, Y. Wu, J. Cong, J. Luo, X. Liu, *Sensors Actuators B: Chem* **2018**, *259*, 1.
- [63] A. Kugimiya, T. Mukawa, T. Takeuchi, *Analyst* **2001**, *126*, 772.
- [64] A. Salimi, M. Roushani, *Electrochem. Commun.* **2005**, *7*, 879.
- [65] X. Qi, R. F. Tester, *Clinical nutrition ESPEN* **2019**, *33*, 18.
- [66] Z. Han, X. Zhang, H. Yuan, Z. Li, G. Li, H. Zhang, Y. Tan, *J. Power Sources* **2022**, *521*, 230956.
- [67] J. Chen, W.-D. Zhang, J.-S. Ye, *Electrochem. Commun.* **2008**, *10*, 1268.
- [68] P. Bollella, S. Sharma, A. E. Cass, F. Tasca, R. Antiochia, *Catalysts* **2019**, *9*, 580.
- [69] Y.-M. Uang, T.-C. Chou, *Biosens. Bioelectron.* **2003**, *19*, 141.
- [70] S. Alexander, P. Baraneedharan, S. Balasubrahmanyam, S. Ramaprabhu, *Mater. Sci. Eng. C.* **2017**, *78*, 124.
- [71] W. Zhang, D. Duan, S. Liu, Y. Zhang, L. Leng, X. Li, N. Chen, Y. Zhang, *Biosens. Bioelectron.* **2018**, *118*, 129.
- [72] M. J. Russo, M. Han, P. E. Desroches, C. S. Manasa, J. Dennaoui, A. F. Quigley, R. M. Kapsa, S. E. Moulton, R. M. Guijt, G. W. Greene, *ACS Sens.* **2021**, *6*, 1482.
- [73] S. Rajendran, D. Manoj, K. Raju, D. D. Dionysiou, M. Naushad, F. Gracia, L. Cornejo, M. Gracia-Pinilla, T. Ahamad, *Sensors Actuators B: Chem* **2018**, *264*, 27.
- [74] W. Wu, Y. Li, J. Jin, H. Wu, S. Wang, Q. Xia, *Sensors Actuators B: Chem.* **2016**, *232*, 633.
- [75] T. K. Mathew, M. Zubair, P. Tadi, *Blood Glucose Monitoring. In: StatPearls*, StatPearls Publishing, Treasure Island, Florida **2023**.
- [76] E. R. F. Collaboration, *Lancet* **2010**, *375*, 2215.
- [77] P. R. Miller, R. M. Taylor, B. Q. Tran, G. Boyd, T. Glaros, V. H. Chavez, R. Krishnakumar, A. Sinha, K. Poorey, K. P. Williams, *Commun. Biology* **2018**, *1*, 173.
- [78] P. P. Samant, M. M. Niedzwiecki, N. Raviele, V. Tran, J. Mena-Lapaix, D. I. Walker, E. I. Felner, D. P. Jones, G. W. Miller, M. R. Prausnitz, *Sci. Transl. Med.* **2020**, *12*, eaaw0285.
- [79] J. P. Bantle, W. Thomas, *J. Clin. Lab. Anal.* **1997**, *130*, 436.
- [80] T. Siegmund, L. Heinemann, R. Kolassa, A. Thomas, *J. Diabetes Sci. Technol.* **2017**, *11*, 766.
- [81] T. Saha, R. Del Caño, K. Mahato, E. De la Paz, C. Chen, S. Ding, L. Yin, J. Wang, *Chem. Rev.* **2023**, *123*, 7854.